


## Research Article

# Experimental Investigation on Proppant Transport Behavior in Hydraulic Fractures of Tight Oil and Gas Reservoir

Guoliang Liu,<sup>1</sup> Shuang Chen,<sup>2</sup> Hongxing Xu,<sup>1</sup> Fujian Zhou,<sup>2</sup> Hu Sun,<sup>1</sup> Hui Li ,<sup>2</sup>  
Zuwen Wang,<sup>1</sup> Xianwen Li,<sup>1</sup> Kaoping Song,<sup>2</sup> Zhenhua Rui,<sup>2</sup> and Ben Li <sup>2</sup>

<sup>1</sup>National Engineering Laboratory for Exploration and Development of Low-Permeability Oil and Gas Fields, Xi'an 710018, China

<sup>2</sup>China University of Petroleum (Beijing), Beijing 102249, China

Correspondence should be addressed to Ben Li; [benli2596@hotmail.com](mailto:benli2596@hotmail.com)

Received 9 November 2021; Revised 7 February 2022; Accepted 9 March 2022; Published 24 March 2022

Academic Editor: Bi Jing

Copyright © 2022 Guoliang Liu et al. This is an open access article distributed under the Creative Commons Attribution License, which permits unrestricted use, distribution, and reproduction in any medium, provided the original work is properly cited.

Proppant concentration and fracture surface morphology are two significant fractures that can affect proppant transport and deposition behavior especially in tight and oil and gas reservoirs. This paper proposed a new set of similarity criteria for proppant experimental design by incorporating proppant concentration and fracture roughness. Based on the proposed criterion, proppant transport experiments in hydraulic fractures of tight oil and gas reservoirs were conducted to explore the proppant placement behavior and identify the key parameters that affected the fracture propping efficiency. Results showed that the proposed similarity criterion can be used to evaluate the onsite proppant transport behavior and optimize hydraulic fracturing parameters. Results showed that the fracture placement efficiency of LD C7 tight oil reservoir is mainly affected by sand ratio and fracturing fluid viscosity. The sand ratio in the LD C7 tight oil reservoir should not be less than 8%, and the optimal carrying fluid viscosity is 5 mPa s. The proppant placement efficiency of the SLG H8 tight gas reservoir is mainly affected by the displacement rate and frac fluid viscosity. The displacement rate of SLG H8 tight gas reservoir should not be less than 3.5 m<sup>3</sup>/min, and the optimal carrying fluid viscosity is 15 mPa s.

## 1. Introduction

In recent years, the hydrocarbon production from conventional oil and gas reservoirs has been reduced dramatically and some of the reservoirs were depleted due to uneconomical production rate. However, the production of unconventional oil and gas reservoirs has been enhanced significantly with the technical innovation of horizontal well drilling and hydraulic fracturing. The objective of hydraulic fracturing is to create a low fluid flow resistance channel, usually called hydraulic fracture, thus enhancing hydrocarbon productivity from the rock matrix. After fracture initiation, proppants are added to frac fluid and pumped to support the fracture open thus reducing hydrocarbon flow resistance. More and more oil and gas companies realized the importance of hydraulic fracturing on the economic exploitation of unconventional oil and gas. If the fracture width and the total sand volume are the same, the propped fracture area should be

the same. However, the shape of the proppant dune should be different. For the tight oil and gas reservoir, the matrix permeability is extremely low (<1 mD), and the primary objective of hydraulic fracturing is to create a longer propped fracture with a lower propped height to promote the tight oil and gas productivity. For conventional oil and gas reservoir, the matrix permeability is relative higher (>10 mD), and the primary objective of hydraulic fracturing is to create a shorter fracture with a higher propped height to bypass the permeability damage section near the wellbore. Reducing flow resistance can be achieved by effective proppant placement. The proppant placement efficiency is affected by numerous factors such as fracture morphology, proppant concentration, slurry rate, viscosity, proppant density, and size. Proppant transport behavior in the fracture has been investigated by numerous scholars experimentally, theoretically, and numerically. Kern et al. [1] designed vertical narrow troughs and conducted proppant transport experiments.

Babcock et al. [2] and Fredrickson and Broaddus [3] suggested to use two parallel transparent plexiglass plates as proppant migration and settlement experimental devices. Schols and Visser [4] introduced a high-speed camera system to record proppant transport behavior. Vlis et al. [5] studied the effect of frac fluid viscosity and proppant size on the proppant settlement and migration behavior in fractures using a visualized flat plate. Sievert et al. [6] evaluated the influence of proppant concentration and multiproppant interaction on the proppant placement behavior in fractures. Roodhart [7] evaluated the effect of the slurry rate on the proppant settlement and migration mechanism. Abdulrahman [8] took the fracture width into consideration. Barree and Conway [9] found that the filtration of frac fluid could affect the settlement and migration process of proppant in fractures. Liu and Sharma [10] studied the effect of fingering phenomenon on proppant transport behavior. Dayan et al. [11] designed a narrow-fracture equipment and investigated proppant transport behavior in shale reservoirs. Li et al. [12] explored the effect of different proppant densities on proppant sedimentation. Wen et al. [13] published a fracturing simulator that could simulate the proppant transport behavior numerically. Guo et al. [14] proposed a large-scale fracture transport device to simulate the proppant settling behavior. Du et al. [15] used the prop fracture length as a key factor to explore the settlement and migration mechanism with frac fluid type and pumping schedule considered. Cheng and Zhou [16] published an extended finite element method framework to evaluate frictional contact on crack slip. Zhan et al. [17] designed a complex fracture experimental device which could simulate “X”, “Y”, “T”, and “H” shape fractures. In order to simulate proppant transport behavior with more factors considered, the scale of proppant transport evaluation apparatus is becoming larger and more complex. Zhang et al. [18] used a pulse plug sand pumping schedule to simulate the settlement behavior in a single fracture; proppant size and size combinations were also considered. He [19] further studied the effect of perforation density and phase angle on the proppant settlement efficiency. The published experimental results and theoretical models can help to guide hydraulic fracturing design, promote hydrocarbon production, and maximize economic benefits. Cheng and Zhou [20, 21] proposed an energy-based criterion of crack branching and conducted numerical simulation to evaluate the dynamic frictional contact problem.

However, the relationship between the indoor proppant transport experimental parameters and onsite hydraulic fractures has not been throughout investigated. Sahai et al. used equal flow rates as the similarity standard to study the proppant settlement and migration process. Hu [22] suggested to conduct proppant transport experiments using the same flow pattern and flow rate as the onsite fracturing process. Li [23] suggested that the Froude number and Reynolds number of the indoor experiment should be equal to those of the onsite hydraulic fracture operations. Sinkov et al. [24] pointed that the proppant to fracturing fluid density ratio should be considered when calculating the Froude number.

Numerous researchers have published their experimental results and similarity criterion on the proppant behavior in the designed fractures. Most of the published papers

focused on the theoretical proppant transport mechanics without the onsite hydraulic fracture operation condition and parameters. It is crucial to establish a reliable proppant transport similarity criterion to ensure that the indoor experiment can simulate the onsite proppant transport process. In order to reveal the true proppant transport behavior, the similarity criterion should ensure that the indoor proppant transport experiment can be represented to the onsite proppant transport operations. In this case, some factors such as flow regime, fracture geometry, and proppant settling time along the fracture and proppant kinematic must be taken into account simultaneously. The novelty of this paper is to propose integrated similarity criterion and conduct serious indoor experiments to reveal the proppant transport behavior of tight oil and gas reservoir. Based on this criterion, onsite proppant transport parameters can be converted into indoor experimental parameters thus evaluating the proppant placement efficiency.

## 2. Similarity Criterion

The proposed similarity criterion includes five factors which are fracture geometric similarity factor, proppant settling velocity similarity factor, proppant Reynolds number similarity factor, fluid Reynolds number similarity factor, and particle Froude number similarity factor. The fracture geometric similarity factor is used to design the indoor fracture geometric parameter (fracture width and length) which can simulate the onsite hydraulic fracture geometry; the proppant settling velocity similarity factor is used to simulate the proppant transport time along the onsite hydraulic fracture; the proppant Reynolds number similarity factor is used to simulate the proppant kinematic during the process of proppant transport; the fluid Reynolds number similarity factor is used to simulate the fluid flow regime of the onsite flow regime; the particle Froude number similarity factor is used to simulate the relationship between the onsite proppant transports in the horizontal and vertical direction. It is crucial to ensure that all the indoor experimental parameters are satisfied with the onsite hydraulic fracturing condition. In this case, similarity ratios are proposed to justify the indoor experimental parameters. The similarity ratio is defined as the ratio between the indoor experimental factors to the onsite hydraulic fracturing operation factor. If all the similarity ratios of the five factors are all in the range of 0.9 to 1.1, the indoor experimental parameters are satisfied to the corresponding onsite hydraulic fracturing operations. The specific similarity ratios of the proposed similarity factors are listed as follows.

Fracture geometric similarity ratio is calculated as follows:

$$F_g = \frac{L}{l} = \frac{H}{h}, \quad (1)$$

where  $L$  and  $H$  represent the length and height of the real fracture, respectively (unit: m) and  $l$  and  $h$  are the length and height of indoor simulated fractures, respectively (m).

The proppant settling velocity similarity ratio is used to confirm that the horizontal velocity to vertical velocity

proportion of the indoor experiment is similar to that of the onsite hydraulic fracturing operation.

Proppant settling velocity similarity ratio is calculated as follows:

$$F_{\text{set}} = \frac{F_{\text{onsite}}}{F_{\text{indoor}}} = \frac{LhV_{s\text{-onsite}}V_{l\text{-indoor}}}{LhV_{s\text{-indoor}}V_{l\text{-onsite}}}, \quad (2)$$

where  $F_{\text{onsite}}$  is the ratio of the time required for the proppant to move one unit horizontal distance to the time required for the proppant to move one unit vertical distance in the real fracture.  $F_{\text{indoor}}$  is the ratio of the time required for the proppant to move one unit horizontal distance to the time required for the proppant to move one unit vertical distance in the experimental fracture.  $V_{s\text{-onsite}}$  is the settlement velocity of proppant particles in the real fracture (m/s).  $V_{s\text{-indoor}}$  is the settlement velocity of proppant particles in the experimental fracture (m/s).  $V_{l\text{-onsite}}$  is the horizontal migration rate of proppant particles in the real fracture (m/s).  $V_{l\text{-indoor}}$  is the horizontal migration rate of proppant particles in the experimental fracture (m/s).

Proppant Reynolds number similarity ratio is calculated as follows:

$$F_{\text{pRe}} = \frac{\text{Re}_{s1}}{\text{Re}_{s2}} = \frac{\rho_1 v_{\text{onsite}} d_1 / \mu_1}{\rho_2 v_{\text{indoor}} d_2 / \mu_2}, \quad (3)$$

where  $\text{Re}_{s1}$  and  $\text{Re}_{s2}$  are the Reynolds numbers of proppant particles in real fracture and simulated fracture, respectively.  $\rho_1$  and  $\rho_2$  are the real fracture fracturing fluid density and simulated fracture fracturing fluid density, respectively ( $\text{kg}/\text{m}^3$ ).  $v_{\text{onsite}}$  and  $v_{\text{indoor}}$  are the true velocity of proppant particle in the real fracture and the true velocity of proppant particle in the simulated fracture, respectively (m/s).  $d_1$  and  $d_2$  are the proppant particle size in the real fracture and proppant particle size in the simulated fracture, respectively (m).  $\mu_1$  and  $\mu_2$  are the real fracture fracturing fluid viscosity and simulated fracture fracturing fluid viscosity, respectively (mPa s).

Fluid Reynolds number similarity ratio is calculated as follows:

$$F_{\text{lRe}} = \frac{\text{Re}_{l1}}{\text{Re}_{l2}} = \frac{\rho_1 v_{\text{onsite}} (4Hw_{\text{onsite}}/2(H+w_{\text{onsite}})) / \mu_1}{\rho_2 v_{\text{indoor}} (4hw_{\text{indoor}}/2(h+w_{\text{indoor}})) / \mu_2}, \quad (4)$$

where  $\text{Re}_{l1}$  and  $\text{Re}_{l2}$  are the Reynolds numbers of fracturing fluids in the real fracture and in the simulated fracture, respectively.  $v_{\text{onsite}}$  and  $v_{\text{indoor}}$  are the flow rates of fracturing fluid in the real fracture and in the simulated fracture, respectively (m/s).  $w_{\text{onsite}}$  and  $w_{\text{indoor}}$  are the fracture widths of the real fracture and the simulated fracture, respectively (m).

Proppant Froude number similarity ratio is calculated as follows:

$$F_{\text{Fr}} = \frac{\text{Fr}_1}{\text{Fr}_2} = \frac{v_{\text{onsite}} / \sqrt{gd_1}}{v_{\text{indoor}} / \sqrt{gd_2}}, \quad (5)$$

where  $\text{Fr}_1$  and  $\text{Fr}_2$  are the Froude numbers of the proppant in the real fracture and in the simulated fracture, respectively.  $g$  is the acceleration of gravity ( $\text{m}/\text{s}^2$ ).

Fracture wall morphology correction coefficient and proppant concentration correlation coefficient were also considered, which can be calculated by the correction equation proposed by Novotny [25]. With all the proposed similarity factors, the accuracy of the simulated proppant transport process experiment is more reliable and the result can be more credible.

The proppant concentration correction coefficient can be calculated as follows [26]:

$$f_C = \frac{1-C}{10^{1.82C}}, \quad (6)$$

where  $f_C$  is the proppant concentration correction coefficient.  $C$  is the proppant concentration (%).

The fracture wall morphology correction coefficient can be calculated as follows [27]:

$$h_w = 0.563 \left( \frac{d_p}{w} \right)^2 - 1.563 \left( \frac{d_p}{w} \right) + 1, \quad (7)$$

where  $h_w$  is the fracture wall morphology correction coefficient.  $d_p$  is the proppant diameter (m).  $w$  is the fracture width (m).

### 3. Proppant Transport Experiments

**3.1. Experimental Apparatus.** The proppant transport experiment was conducted with a large-scale visual sand-carrying migration evaluation apparatus, which was composed of six parts, including pumping system, visual fracture, sand-mixing tank, circulation system, sand washing system, and an electronic control system, as shown in Figure 1. The maximum displacement rate of the centrifugal pump can be  $8 \text{ m}^3/\text{min}$ , which fully meets the requirements of frac fluid pumping rate. The visual fracture is composed of 10 transparent parallel plexiglass plates. The overall length of the fracture is 2.5 m, and the height of the fracture is 0.5 m, and the width of the fracture is 4 mm. The inlet and outlet sections of the proppant transport experimental apparatus are shown in Figure 1(c).

**3.2. Experimental Design and Material Preparation.** The proposed similarity criterion has been coded via Excel and the proposed similarity ratio can also be calculated. The proposed five similarity ratios can be calculated to meet the similarity criterion. The programmed calculation spreadsheet is shown in Table 1. The hydraulic fracturing onsite operation parameters are included and taken as an example to explain the design of the indoor experimental parameters. From Table 1, the fracture geometry similarity ratio is 0.96, the proppant settling velocity similarity ratio is 1.08, the proppant Reynolds number similarity ratio is 1.07, the fluid Reynolds number similarity ratio is 1.08, and the proppant Froude number similarity ratio is 0.95. All the proposed similarity ratios are laid in between 0.9 and 1.1, indicating that

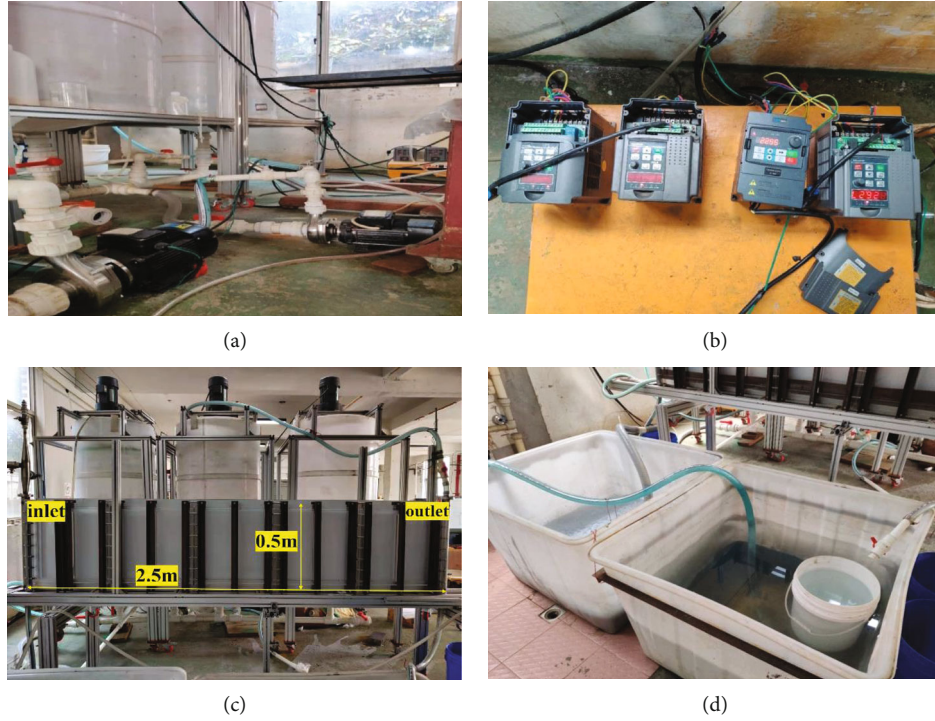


FIGURE 1: The physical diagram of the large-scale visual sand-carrying migration evaluation device: (a) centrifugal pump, (b) control system, (c) visual fractures, sand-mixing tank, and circulation system, and (d) sand washing system.

TABLE 1: Programmed similarity criterion (example LD C7).

Parameter	Onsite	Indoor	Unit
Fracture length	$2.40E + 02$	$2.50E + 00$	m
Fracture height	$5.00E + 02$	$5.00E - 01$	m
Fracture width	$8.00E - 03$	$4.00E - 03$	mm
Fracture velocity	$1.88E - 01$	$1.40E - 01$	m/s
Frac fluid density	$1.00E + 03$	$1.00E + 03$	kg/m <sup>3</sup>
Frac fluid viscosity	$5.00E - 03$	$2.00E - 03$	mPa s
Proppant density	$2.42E + 03$	$2.31E + 03$	kg/m <sup>3</sup>
Proppant diameter	$1.65E - 04$	$8.30E - 05$	μm
Sand ratio	$5.70E - 02$	$1.00E - 02$	%
Proppant settling velocity	$1.66E - 02$	$8.61E - 03$	m/s
Fracture roughness factor	$9.68E - 01$	$9.68E - 01$	
Proppant concentration coefficient	$7.43E - 01$	$9.49E - 01$	
Ture settling velocity	$1.19E - 02$	$7.91E - 03$	m/s
Ture horizontal velocity	$1.88E - 01$	$1.40E - 01$	m/s
Flow rate	$4.50E + 00$	$1.68E - 02$	m <sup>3</sup> /min
Frac fluid Reynolds number	$6.00E - 01$	$5.56E - 01$	
Proppant Reynolds number	$6.20E + 00$	$5.82E + 00$	
Proppant Froude number	$1.46E - 02$	$1.54E - 02$	
Proppant settling velocity	$3.05E - 01$	$2.83E - 01$	
Fracture geometry	$4.8E + 01$	$5.0E + 01$	



TABLE 2: Evaluation experiment scheme of LD C7.

Experiment no.	Displacement rate	Viscosity		Sand ratio	Particle size and density (quartz sand)	
	Field m <sup>3</sup> /min	Field mPa s	Indoor mPa s	Field %	Field Mesh	Indoor Mesh
1	5.6	6	2	6.0	100	180
	4.8	6	2	6.0	40/70	120/140
	4.8	6	2	6.0	20/40	40/70
2	3.7	14	5	6.0	100	180
	3.7	14	5	6.0	40/70	120/140
	3.7	14	5	6.0	20/40	40/70
3	4.5	5	2	5.7	100	180
	4.5	5	2	15.8	40/70	120/140
	4.5	13	5	24.6	20/40	40/70
4	3.0	5	2	5.7	100	180
	3.0	5	2	15.8	40/70	120/140
	3.0	13	5	24.6	20/40	40/70

TABLE 3: Displacement rate exploration experiment scheme of LD C7.

Experiment no.	Displacement rate	Viscosity		Sand ratio	Particle size and density (quartz sand)	
	Field m <sup>3</sup> /min	Field mPa s	Indoor mPa s	Field %	Field Mesh	Indoor Mesh
CD1	4.5	5	2	5.7	100	180
	4.5	5	2	15.8	40/70	120/140
	4.5	14	5	24.6	20/40	40/70
CD2	3.0	5	2	5.7	100	180
	3.0	5	2	15.8	40/70	120/140
	3.0	13	5	24.6	20/40	40/70

the indoor experimental parameters can be used to simulate the onsite hydraulic fracturing process. It is crucial to be noticed that the designed indoor parameters are not unique; some parameters such as fracture velocity, proppant diameter, and fluid density can be changed for the indoor experimental design. The designed indoor parameters must be dependent on the physical reliable range and availability of the experimental materials. In the previous proppant experimental design, it is preferred that the sand and fluid used in slot tests should be the same to the field designs. This will ensure the same proppant settling velocity and drag force applied to the particles. However, some other similarity ratios of other factors such as proppant Froude number and proppant Reynolds number cannot be met. The proposed similarity criterion can solve this problem.

In this paper, the proppant transport behavior of LD C7 tight oil formation and the SLG H8 tight gas formation of CQ oilfield in China was taken as an example. According to the hydraulic fracturing operation parameters, a series of indoor experiments were conducted. The experiments include field evaluation experiments and parameter optimization experiments. All the indoor experimental parameters were designed by the proposed similarity criterion. The field

evaluation experiments were used to reveal the currently proppant placement behavior while the optimization experiments were conducted to identify the key factors that could contribute to the proppant placement behavior. The field operation parameters and designed experimental parameters of LD C7 and SLG H8 are showed in Tables 2–8.

In the field evaluation experiments, in order to simulate the field proppant transport and settling behavior, the field proppant slurry pumping schedule was used. The field proppant and fracturing fluid volume were scaled to the indoor experimental parameters. Other indoor experimental parameters were designed based on the proposed similarity criterion. In the parameter optimization experiments, proppant was designed by changing the displacement rate, proppant size, proppant concentration, and frac fluid viscosity. The proppants used in the indoor experiments include 40-70 mesh quartz sand with a density of 2537 kg/m<sup>3</sup>, 120~140 mesh quartz sand with a density of 2393 kg/m<sup>3</sup>, 180 mesh quartz sand with a density of 2308 kg/m<sup>3</sup>, 40~70 mesh ceramic with a density of 2668 kg/m<sup>3</sup>, and 100-140 mesh ceramic with a density of 2565 kg/m<sup>3</sup>. The fracturing fluid viscosities are 2 mPa s, 3 mPa s, 5 mPa s, 8 mPa s, and 11 mPa s.

TABLE 4: Sand concentration exploration experiment scheme of LD C7.

Experiment no.	Displacement rate	Viscosity		Sand ratio	Particle size and density (quartz sand)	
	Field m <sup>3</sup> /min	Field mPa s	Indoor mPa s	Field %	Field Mesh	Indoor Mesh
CS1	4.8	6	2	6.0	20/40	40/70
CS2	4.8	5	2	8.0	20/40	40/70
CS3	4.8	5	2	6.0	40/70	120/140
CS4	4.8	5	2	8.0	40/70	120/140

TABLE 5: Fracturing fluid viscosity exploration experimental scheme of LD C7.

Experiment no.	Displacement rate	Viscosity		Sand ratio	Particle size and density (quartz sand)	
	Field m <sup>3</sup> /min	Field mPa s	Indoor mPa s	Field %	Field Mesh	Indoor Mesh
CV1	4.8	3	1	6.0	20/40	40/70
CV2	4.8	5	2	8.0	20/40	40/70
CV3	4.8	6	2	6.0	20/40	40/70
CV4	4.4	9	3	8.0	20/40	40/70
CV5	4.5	14	5	24.6	20/40	40/70
CV7	4.1	30	11	8.0	20/40	40/70
CV8	4.8	3	1	6.0	40/70	120/140
CV9	4.8	5	2	8.0	40/70	120/140
CV10	4.4	9	3	8.0	40/70	120/140
CV11	4.9	14	5	8.0	40/70	120/140

TABLE 6: Evaluation experiment scheme of SLG H8.

Experiment no.	Displacement rate	Viscosity		Sand ratio	Particle size and density (quartz sand)	
	Field m <sup>3</sup> /min	Field mPa s	Indoor mPa s	Field %	Field Mesh	Indoor Mesh
H1	4.5	15	5	20	40/70	100/140
	4.5	15	5	20	20/40	40/70
H2	3.5	15	5	20	40/70	100/140
	3.5	15	5	20	20/40	40/70

TABLE 7: Displacement rate exploration experiment scheme of SLG H8.

Experiment no.	Displacement rate	Viscosity		Sand ratio	Particle size and density (quartz sand)	
	Field m <sup>3</sup> /min	Field mPa s	Indoor mPa s	Field %	Field Mesh	Indoor Mesh
HD1	4.5	15	5	20	40/70	100/140
	4.5	15	5	20	20/40	40/70
HD2	3.5	15	5	20	40/70	100/140
	3.5	15	5	20	20/40	40/70

TABLE 8: Fracturing fluid viscosity exploration experimental scheme of SLG H8.

Experiment no.	Displacement rate	Viscosity		Sand ratio	Particle size and density (quartz sand)	
	Field m <sup>3</sup> /min	Field mPa s	Indoor mPa s	Field %	Field Mesh	Indoor Mesh
HV1	4.5	15	5	20	20/40	40/70
HV2	3.5	15	5	20	40/70	100/140
HV3	3.5	24	8	20	40/70	100/140

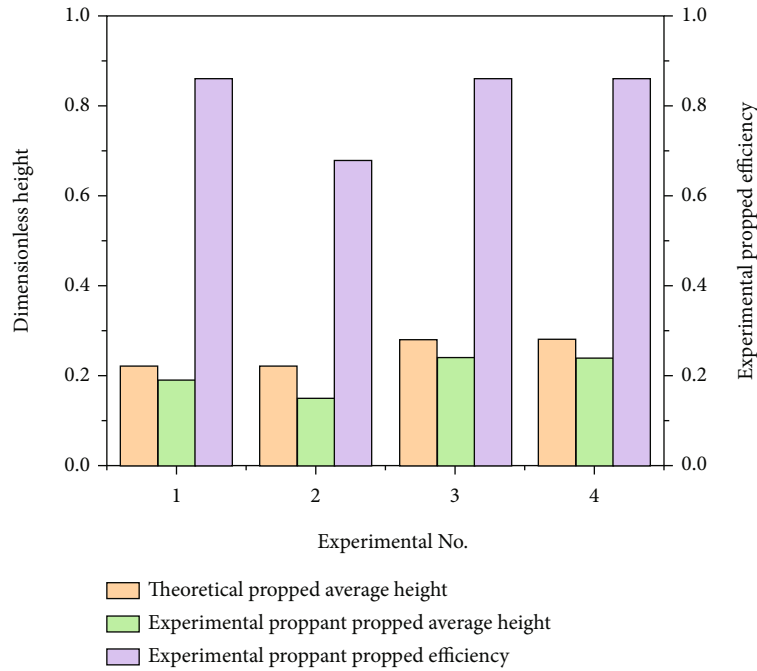


FIGURE 2: Comparison of current parameter placement results.

#### 4. Experimental Results and Analysis of LD C7

The indoor experiment investigated the characteristics of proppant transport and placement under the current hydraulic fracturing operation parameters of LD C7 tight oil formation and evaluated the effect of pumping rate, proppant concentration, and frac fluid viscosity on the proppant placement efficiency. The height and sand dune shape for each experiment were recorded and analyzed.

*4.1. Characteristics of Proppant Transport and Placement under Current Fracturing Parameters.* Some parameters, including experimental proppant propped area, theoretical propped area, and proppant placement efficiency, were introduced and defined to evaluate the proppant transport behavior. The experimental proppant propped area is defined as the area of the proppant settled in the experimental fracture, while the theoretical propped area is defined as the pumped proppant volume divided by the experimental fracture width. The proppant placement efficiency is defined as the ratio of experimental proppant propped area to the theoretical propped area, which is an indicator of the proppant propped efficiency. The proppant placement efficiency

under a variety of in situ fracturing parameters (experiments in Table 2) was explored, and the summarized dimensionless height results are shown in Figure 2. The dimensionless height is defined as the ratio of the experimental proppant propped average height to the theoretical propped average height. It can be seen that the proppant placement efficiency of experiments no. 1 to 4 was ranged from 0.68 to 0.86. The difference between the experimental proppant propped efficiency and the theoretical propped efficiency (is equal to 1) was calculated. For example, the experimental proppant propped efficiency of experiment no. 1 is 0.86, and the theoretical propped efficiency is 1, so the difference between the experimental proppant propped efficiency and the theoretical propped efficiency of experiment no. 1 is 0.14. It can be seen from Figure 2 that the difference range between the experimental proppant propped efficiency and the theoretical propped efficiency of experiments no. 1 to 4 is from 0.32 to 0.14, which proved that the onsite proppant placement was effective to some extent. Further experiments were conducted to optimize the fracture placement efficiency.

*4.2. Effect of Displacement Rate on Proppant Placement.* The displacement rate of experiment no. CD1 is 4.5 m<sup>3</sup>/min, and

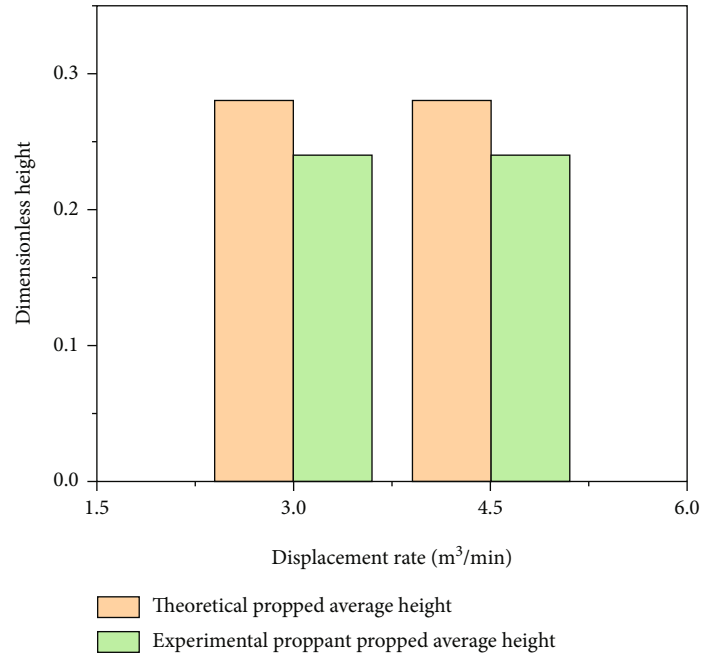


FIGURE 3: Comparison of different displacement rate placement results.

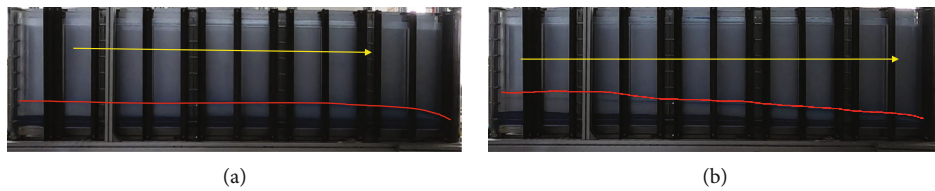


FIGURE 4: Layout diagram of sand dune with different displacement rates: (a) displacement rate of 4.5 m<sup>3</sup>/min and (b) displacement rate of 3 m<sup>3</sup>/min.



FIGURE 5: Layout diagram of sand dune with different sand ratios: (a) sand ratio of 6% and (b) sand ratio of 8%.

the displacement rate of experiment no. CD2 is 3.0 m<sup>3</sup>/min, while the fracturing fluid viscosity, sand ratio, and injection volume were kept constant. By comparing the experimental results of no. CD1 and no. CD2, it is found that within the operation displacement rate range of LD C7 tight oil formation, displacement rate does not affect the proppant placement efficiency in the fracture; however, it can affect the shape of the sand dune, as shown in Figures 3 and 4. If the proppant is pumped at a low displacement rate, more proppant will be deposited in the fracture near the wellbore, which will lead to a large amount of fracture area unpropped in the fracture far away from the wellbore. Therefore, it should be better to choose a relatively higher displacement rate to increase the fracture propping efficiency while keeping the displacement rate in the operation available range.

**4.3. Effect of Proppant Concentration on Proppant Placement.** Proppant concentration is one of the important parameters that can affect the efficiency of proppant placement. High proppant concentration can help to transport more proppant in the fractures and enhance the fracture propping efficiency; however, the risk of wellbore blockage or sand-out would also be high. For LD C7 tight oil formation, we conducted some experiments to figure out the lower limit of the proppant concentration for 20/40 mesh and 40/70 mesh quartz sand. Figure 5 shows the dimensionless height of 40/70 mesh quartz sand placement results under the proppant conditions of 6% and 8%. As shown in Figure 6, for proppant concentration of 6%, the dimensionless height formed by 20/40 mesh quartz sand is 0.19, while for proppant concentration of 8%, the dimensionless height is 0.36. The dimensionless height of 8%



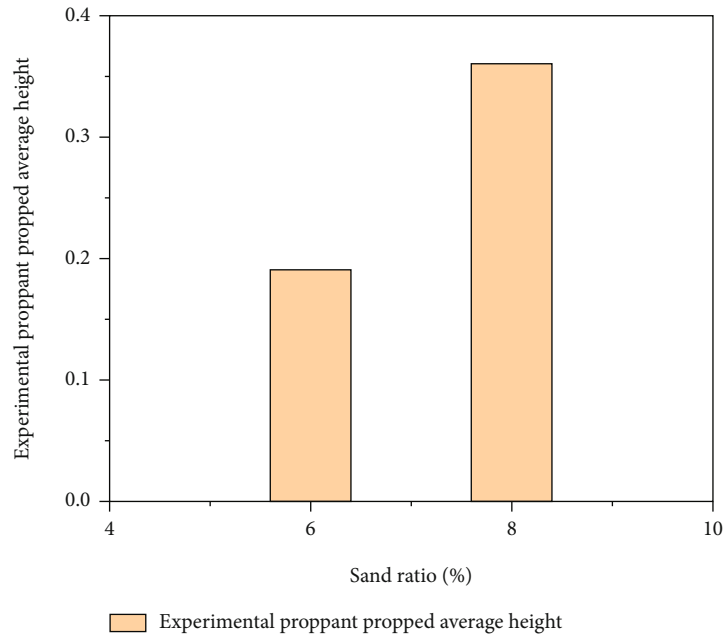


FIGURE 6: Comparison diagram of 20/40 mesh quartz sand placement results with different sand ratios.

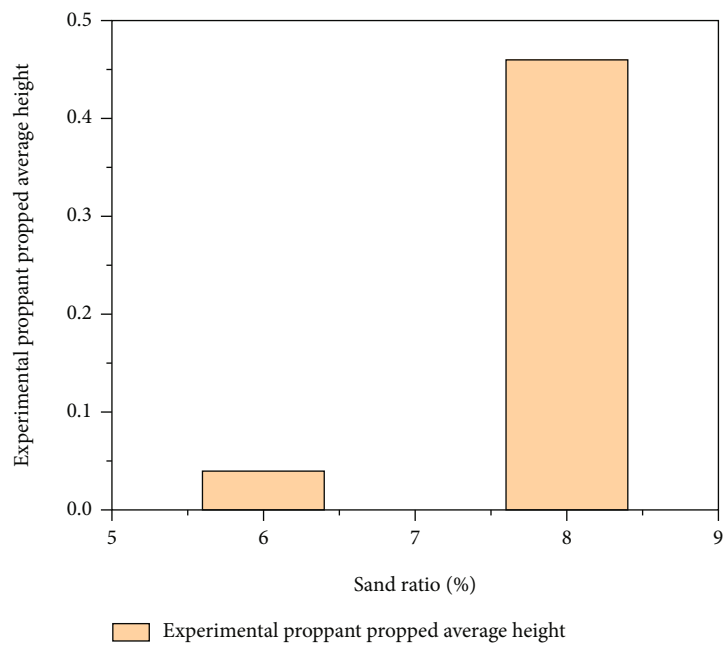


FIGURE 7: Comparison of 40/70 mesh quartz sand placement results with different sand ratios.

20/40 mesh quartz sand was almost two times higher than that of 6% 20/40 mesh quartz sand. Therefore, for 20/40 mesh quartz sand, the proppant concentration should be no less than 8%.

Figure 7 shows the dimensionless height of 40/70 mesh quartz sand placement results under the proppant conditions of 6% and 8%. For 6% proppant concentration, the propped height is zero, while for 8% proppant concentration, the dimensionless height is 0.46, which is also shown

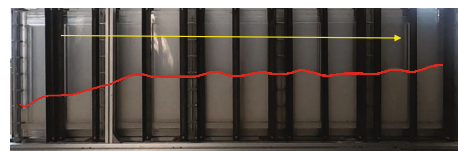


FIGURE 8: Embankment configuration of 40/70 mesh quartz sand with 8% sand ratio.

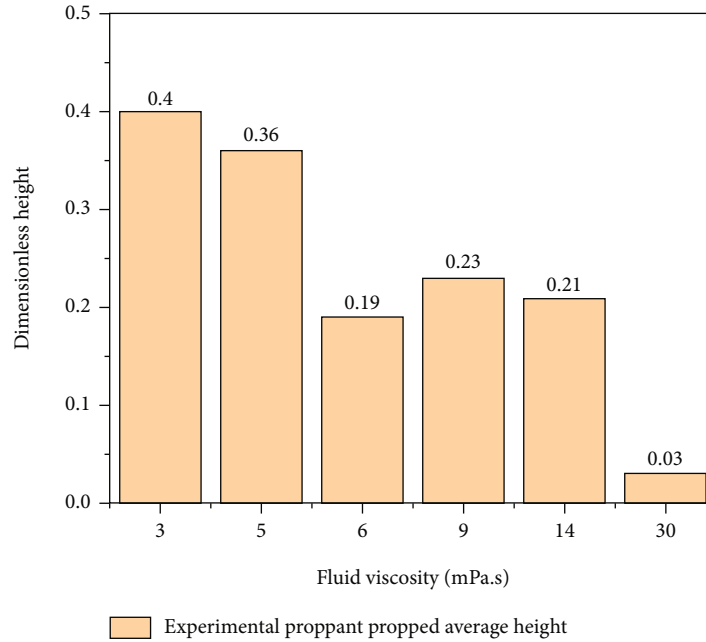


FIGURE 9: Comparison of 20/40 mesh quartz sand placement results with different fracturing fluid viscosities.



FIGURE 10: Configuration of 20/40 mesh quartz sand with different fracturing fluid viscosities: (a) viscosity of 3 mPa s and (b) viscosity of 5 mPa s.

in Figure 8. Therefore, for the 40/70 mesh quartz sand, the proppant concentration should be no less than 8%.

**4.4. Effect of Fluid Viscosity on Proppant Placement.** The viscosity of fracturing fluid is also one of the most important factors that could affect proppant placement efficiency. We conducted comparison experiments of 20/40 mesh quartz sand with frac fluid viscosity of 3 mPa s, 5 mPa s, 6 mPa s, 9 mPa s, 14 mPa s, and 30 mPa s. Dimensionless height of these experiments is shown in Figure 9. When the fracturing fluid viscosity is 3 mPa s, the dimensionless height of the sand dune is 0.4 (the highest). When the fracturing fluid viscosity is 5 mPa s, 6 mPa s, and 9 mPa s, the height of the sand dune is 0.36, 0.19, and 0.23, respectively. When the fracturing fluid viscosity is 30 mPa s, the dimensionless height is 0.03, indicating that if the frac fluid viscosity is higher than 30 mPa s, the fracture propped efficiency is extremely small. However, compared with the sand dune shape of 3 mPa s and 5 mPa s frac fluid, the 20/40 mesh quartz sand carried by 3 mPa s frac fluid mainly accumulated near the wellbore zone, while 20/40 mesh quartz sand carried by 5 mPa s frac fluid has a more uniform distribution of sandbanks, as shown in Figure 10. Therefore, 5 mPa s is the lower limit vis-

cosity for 20/40 mesh quartz sand. In addition, for 20/40 mesh quartz sand, the optimal carrying liquid viscosity is 5 mPa s. For 40/70 mesh quartz sand, as shown in Figures 11 and 12, the optimal frac fluid viscosity is 5 mPa s.

## 5. Experimental Results and Analysis of SLG H8

The indoor experiment investigated the characteristics of proppant transport and placement under the current hydraulic fracturing operation parameters of SLG H8 tight gas formation and evaluated the effect of pumping rate, proppant concentration, and frac fluid viscosity on the proppant placement efficiency. The height and sand dune shape for each experiment were recorded and analyzed. There are two differences between SLG H8 and LD C7. The fracturing fluid type of LD C7 is slickwater while that of SLH H8 is guar gum fracturing fluid. The proppant type of LD C7 is quartz sand while that of SLG H8 is ceramic.

**5.1. Characteristics of Proppant Transport and Placement under Current Fracturing Parameters.** The proppant placement efficiency under a variety of in situ fracturing parameters (experiment nos. H1 and H2 in Table 6) was explored,

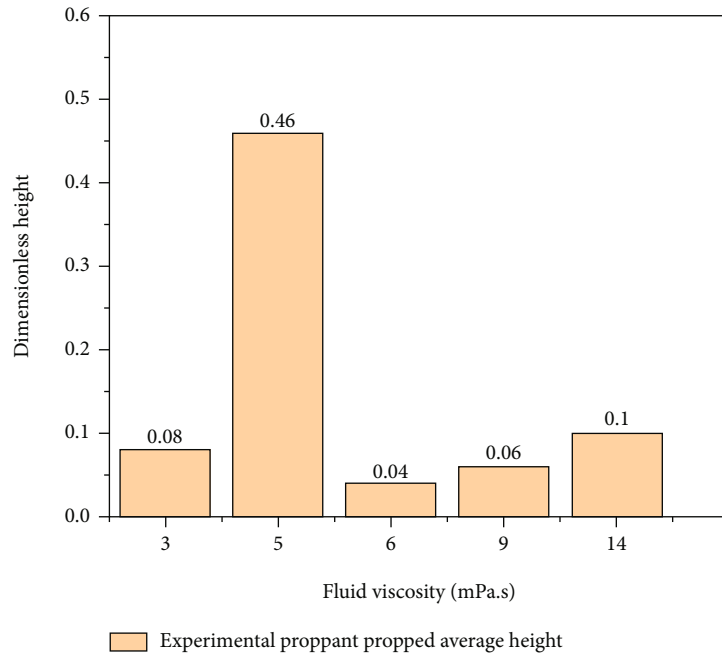


FIGURE 11: Comparison of 40/70 mesh quartz sand placement results with different fracturing fluid viscosities.

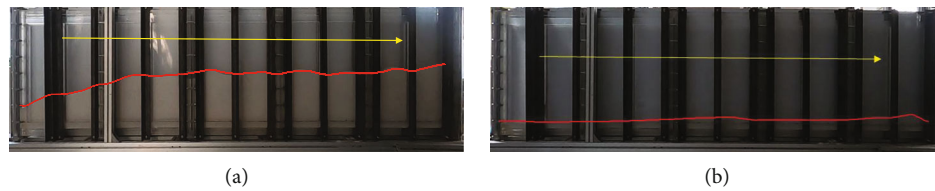


FIGURE 12: Configuration of 40/70 mesh quartz sand with different fracturing fluid viscosities: (a) viscosity of 5 mPa s and (b) viscosity of 14 mPa s.



FIGURE 13: Sand embankment placement morphology in the evaluation experiment of tight gas layer: (a) the 12th group experiment and (b) the 13th group experiment.

and the experimental results are shown in Figure 13. A total of 0.2 fracture volume proppant was pumped into the fracture. It can be seen that the dimensionless heights of experiment nos. H1 to H2 were almost equal to each other. However, the sand dune of the no. H1 experiment has a relatively flat layout, indicating the fracture is nearly uniformly propped from the wellbore to the fracture tip. However, the proppants of 20/40 mesh and 40/70 mesh ceramic in the no. H2 experiment were accumulated higher near the wellbore. Additional experiments should be conducted to optimize the proppant transport parameters.

*5.2. Effect of Displacement Rate on Proppant Placement.* The displacement rate of experiment no. HD1 is  $4.5 \text{ m}^3/\text{min}$ , and the displacement rate of experiment no. HD2 is  $3.5 \text{ m}^3/\text{min}$ , while the fracturing fluid viscosity, sand ratio, and injection volume were kept constant. The experimental results are shown in Figure 14. For the displacement rate of  $4.5 \text{ m}^3/\text{min}$ , the dimensionless height of the ceramic dune within the fracture is 0.16, indicating that the experimental propped height is 80% of the theoretical height. However, for the displacement rate of  $3.5 \text{ m}^3/\text{min}$ , the dimensionless height of the ceramic dune in the fracture is 0.1, indicating that the

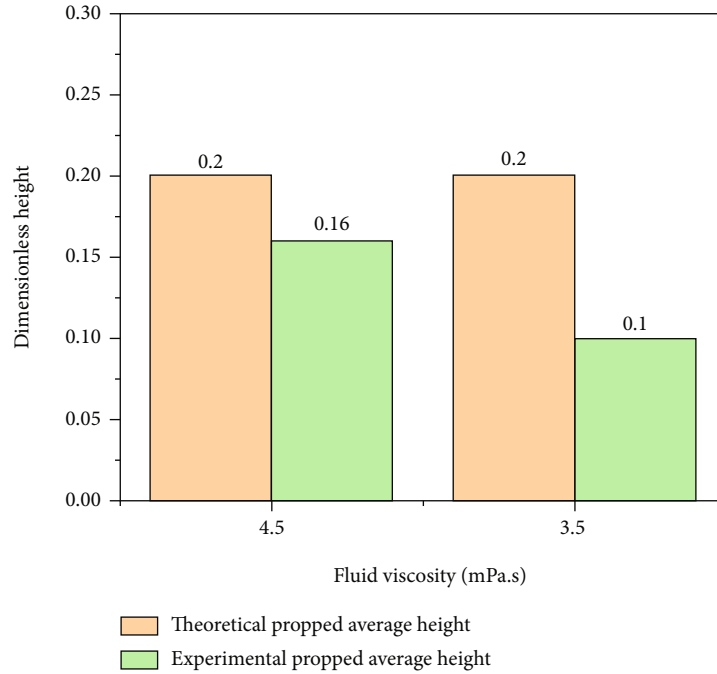


FIGURE 14: Comparison of placement results of ceramic proppant at different displacement rates.



FIGURE 15: 20/40 mesh ceramsite sand embankment configuration with sand-carrying liquid viscosity of 15 mPa s.



FIGURE 16: 40/70 mesh ceramic sand embankment configuration with sand-carrying liquid viscosity of 24 mPa s.

experimental propped height is 50% of the theoretical height. Therefore, a greater flow rate should be used for pumping ceramic proppant, and the recommended proppant displacement rate should be no less than 3.5 m<sup>3</sup>/min.

**5.3. Effect of Frac Fluid Viscosity on Proppant Placement.** We conducted comparison experiments of 20/40 mesh ceramic proppant with frac fluid viscosity of 15 mPa s (experiment nos. HV1, HV2, and HV3). The fracture propping results of experiment no. HV2 are shown in Figure 15. The 15 mPa s frac fluid can provide a relative better fracture propping efficiency. Therefore, the carrying fluid viscosity of 20/40 mesh ceramic proppant is 15 mPa s.

From the proppant placement results of no. HV1 and no. HV2 (Figure 14), it is found that the 40/70 mesh ceramic

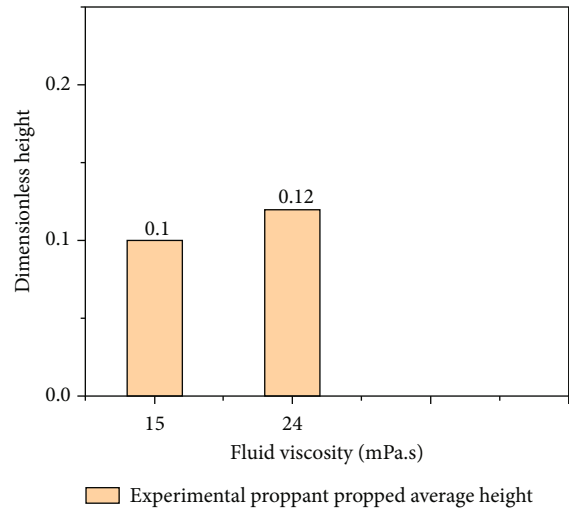


FIGURE 17: Comparison of results of 40/70 mesh ceramic placement with different sand-carrying fluid viscosities.

is mainly placed in the fracture near the wellbore. In order to transport the 40/70 mesh ceramic proppant to the far-field fracture, the viscosity of the fracturing fluid was increased to 24 mPa s (experiment no. HV3), and the proppant placement results of 40/70 mesh ceramic are shown in Figure 16. Comparing the results of experiments no. HV2 and no. HV3 (Figure 17), the dimensionless height would increase as the frac fluid viscosity increased. However, the degree of the dimensionless height increment is 0.02, which is slight and insignificant. In summary, the viscosity of the 40/70 mesh ceramic proppant-carrying fluid should be greater than 15 mPa s.

## 6. Conclusion

This paper proposed a new set of similarity criteria for proppant experimental design by incorporating proppant concentration and fracture roughness. The proposed similarity criterion includes five factors which are fracture geometric similarity factor, proppant settling velocity similarity factor, proppant Reynolds number similarity factor, fluid Reynolds number similarity factor, and particle Froude number similarity factor. Based on the proposed criterion, proppant transport experiments in hydraulic fractures of LD C7 tight oil and H8 gas reservoirs were carried out to explore the proppant placement mechanism and the key parameters that affected the fracture propping efficiency were identified. The following results were obtained:

- (1) This paper proposed a comprehensive similarity criterion and conducted serious indoor experiments to reveal the proppant transport behavior in hydraulic fractures of tight oil and gas reservoir. Based on this criterion, onsite proppant transport parameters were converted into indoor experimental parameters
- (2) The proposed similarity criterion was programmed and serious indoor proppant transport experiments were conducted to evaluate the onsite frac fluid viscosity and sand ratio of LD C7 tight oil. Results showed that the sand ratio in the LD C7 tight oil reservoirs should not be less than 8%, and the optimal carrying fluid viscosity is 5 mPa s
- (3) The proppant placement efficiency in the H8 tight gas reservoir is mainly affected by the displacement rate and frac fluid viscosity. Based on the experimental results, the displacement rate of H8 tight gas reservoir should not be less than 3.5 m<sup>3</sup>/min, and the optimal carrying fluid viscosity is 15 mPa s
- (4) LD C7 tight oil reservoir used quartz sand as a proppant, while H8 tight gas reservoir used ceramic as a proppant. Proppant types and carrying fluid viscosity are the two significant parameters that can affect the proppant transport and placement behavior

## Data Availability

All the data have been provided in the manuscript.

## Conflicts of Interest

The authors declare that they have no conflicts of interest.

## Acknowledgments

This research was supported by the National Natural Science Foundation of China (No. 52004308), by the National Engineering Laboratory for Exploration and Development of Low-Permeability Oil and Gas Fields Foundation of China (No. cqzt-cqjx-2019-zcj-041), and by the National Engineering Laboratory for Drilling Technics of Oil and Gas Foundation of China (No. F2020188).

## References

- [1] L. R. Kern, T. K. Perkins, and R. E. Wyant, "The mechanics of sand movement in fracturing," *Journal of Petroleum Technology*, vol. 11, no. 7, 1959.
- [2] R. E. Babcock, C. L. Prokop, and R. O. Kehle, "Distribution of propping agent in vertical fractures," in *In Drilling and Production Practice*, OnePetro, 1967.
- [3] S. E. Fredrickson and G. C. Broaddus, "Selective placement of fluids in a fracture by controlling density and viscosity," *Journal of Petroleum Technology*, vol. 28, no. 5, 1976.
- [4] R. S. Schols and W. Visser, "Proppant bank buildup in a vertical fracture without fluid loss," in *In SPE European Spring Meeting*, OnePetro, 1974.
- [5] A. C. Van der Vlis, R. Haafkens, B. A. Schipper, and W. Visser, "Criteria for proppant placement and fracture conductivity," in *In Fall Meeting of the Society of Petroleum Engineers of AIME*, OnePetro, 1975.
- [6] J. A. Sievert, H. A. Wahl, P. E. Clark, and M. W. Harkin, "Proppant transport in a large vertical model," in *In SPE/DOE Low Permeability Gas Reservoirs Symposium*, OnePetro, 1981.
- [7] L. P. Roodhart, "Proppant settling in non-Newtonian fracturing fluids," in *In SPE/DOE Low Permeability Gas Reservoirs Symposium*, OnePetro, 1985.
- [8] A. A. Al-quraishi and R. L. Christiansen, "Dimensionless groups for interpreting proppant transport in hydraulic fractures," in *Middle East Oil Show and Conference*, Bahrain, February 1999.
- [9] R. D. Barree and M. W. Conway, "Proppant holdup, bridging, and screenout behavior in naturally fractured reservoirs," in *In SPE Production and Operations Symposium*, OnePetro, 2001.
- [10] Y. Liu and M. M. Sharma, "Effect of fracture width and fluid rheology on proppant settling and retardation: an experimental study," in *In SPE Annual Technical Conference and Exhibition*, OnePetro, 2005.
- [11] A. Dayan, S. M. Stracener, and P. E. Clark, "Proppant transport in slickwater fracturing of shale gas formations," in *In SPE Annual Technical Conference and Exhibition*, OnePetro, 2009.
- [12] X. L. Li, W. Xiao, and K. Wang, "Setting laws of the proppant in VES fracturing fluid," *Petroleum Geology and Oilfield Development in Daqing*, vol. 34, no. 2, pp. 95–98, 2015.
- [13] Q. Z. Wen, X. J. Liu, and B. Huang, "Development and application of hydraulic fracturing visual fracture simulation system," *Special Oil and Gas Reservoirs*, vol. 23, no. 2, pp. 136–139, 2016.
- [14] T. K. Guo, Z. Q. Qu, and M. Z. Li, "Development of the large-scale virtual simulation experimental device of proppant transportation and placement in complex fractures," *Research and Exploration in Laboratory*, vol. 37, no. 10, pp. 242–246, 2018.
- [15] X. F. Du, X. Zhang, and M. R. Tang, "Research on multi-stage pulsed fracturing technology for thin interbeds," *Drilling and Production Technology*, vol. 41, no. 1, pp. 65–68, 2018.
- [16] H. Cheng and X. Zhou, "New technique for frictional contact on crack slip in the extended finite-element method framework," *Journal of Engineering Mechanics*, vol. 144, no. 8, article 4018059, 2018.
- [17] Y. P. Zhan, M. L. Luo, and J. J. Gao, "A proppant migration simulation device with variable mesh structure," *Yangtze University (Natural Science Edition)*, vol. 16, no. 8, pp. 53–57, 2019.



- [18] K. S. Zhang, T. W. Zhang, and S. L. Wu, "Simulation of proppant transport in fracture with different combinations of particle size," *Reservoir Evaluation and Development*, vol. 9, no. 6, pp. 72–77, 2019.
- [19] S. Y. He, *Simulation study on transport law of proppant in complex fractures Master's thesis*, Southwest Petroleum University, Chengdu, Sichuan, China (in Chinese), 2019.
- [20] H. Cheng and X. Zhou, "An energy-based criterion of crack branching and its application on the multidimensional space method," *International Journal of Solids and Structures*, vol. 182-183, pp. 179–192, 2020.
- [21] H. Cheng and X. Zhou, "Numerical simulation of the dynamic frictional contact problem for crack slip based on the multidimensional space method," *Journal of Engineering Mechanics*, vol. 145, no. 2, 2019.
- [22] L. X. Hu, *Method study of optimizing parameters of channel fracturing Master's thesis*, China University of Petroleum (East China), Beijing, China (in Chinese), 2014.
- [23] Z. M. Li, *Laboratory experimental study on proppant transportation in complex fracture network of tight reservoir Master's thesis*, Southwest Petroleum University, Chengdu, Sichuan, China (in Chinese), 2019.
- [24] K. Sinkov, X. Weng, and O. Kresse, "Modeling of proppant distribution during fracturing of multiple perforation clusters in horizontal wells," in *In SPE Hydraulic Fracturing Technology Conference and Exhibition*, OnePetro, 2021.
- [25] E. J. Novotny, "Proppant transport," in *In SPE Annual Fall Technical Conference and Exhibition*, OnePetro, 1977.
- [26] R. J. Clifton and J. J. Wang, "Multiple fluids, proppant transport, and thermal effects in three-dimensional simulation of hydraulic fracturing," in *SPE Annual Technical Conference and Exhibition*, Houston, TX, USA, October 1988.
- [27] P. B. Gadde, Y. Liu, J. Norman, R. Bonnecaze, and M. M. Sharma, "Modeling proppant settling in water-fracs," in *SPE Annual Technical Conference and Exhibition*, Houston, TX, USA, September 2004.